

Evaluating Anomaly Detectors for Simulated Highly Imbalanced Industrial Classification Problems

Lesley Wheat^{*†‡}, Martin v. Mohrenschmidt^{*} and Saeid Habibi[†]

^{*}Department of Computing and Software, McMaster University, Hamilton, Canada

[†]Center for Mechatronics and Hybrid Technologies, McMaster University, Hamilton, Canada

[‡]Email: wheatd@mcmaster.ca

Abstract— Machine learning offers potential solutions to current issues in industrial systems in areas such as quality control and predictive maintenance, but also faces unique barriers in industrial applications. An ongoing challenge is extreme class imbalance, primarily due to the limited availability of faulty data during training. This paper presents a comprehensive evaluation of anomaly detection algorithms using a problem-agnostic simulated dataset that reflects real-world engineering constraints. Using a synthetic dataset with a hyper-spherical based anomaly distribution in 2D and 10D, we benchmark 14 detectors across training datasets with anomaly rates between 0.05% and 20% and training sizes between 1 000 and 10 000 (with a testing dataset size of 40 000) to assess performance and generalization error. Our findings reveal that the best detector is highly dependant on the total number of faulty examples in the training dataset, with additional healthy examples offering insignificant benefits in most cases. With less than 20 faulty examples, unsupervised methods (kNN/LOF) dominate; but around 30-50 faulty examples, semi-supervised (XGBOD) and supervised (SVM/CatBoost) detectors, we see large performance increases. While semi-supervised methods do not show significant benefits with only two features, the improvements are evident at ten features. The study highlights the performance drop on generalization of anomaly detection methods on smaller datasets, and provides practical insights for deploying anomaly detection in industrial environments.

Index Terms—Machine Learning, Class Imbalance, Anomaly Detection, Classification, Monte Carlo Simulation, Synthetic Datasets.

I. INTRODUCTION

With recent advances in machine learning, there has been increasing interest in applying data-driven methods to ongoing industrial challenges such as fault detection, process monitoring, quality control, and more [1], [2], [3], [4]. Data-driven methods offer the potential to automate inspection points, reduce equipment failures and improve overall efficiency, all without requiring expert knowledge of the system in question. However, industrial applications are known to have challenges and considerations that are not present in other machine learning applications, making it difficult to directly translate the results from existing benchmarks to specific use cases [5].

In industrial settings, examples of faulty or defective conditions are often extremely limited due to multiple factors. For example, the anomaly rate in real-world mass manufacturing problems can easily fall under 1% [6], which creates a significant barrier to effectively training machine learning models. While classifiers often struggle in these scenarios, anomaly detection techniques have been formulated for the purpose of tackling these very sorts of extreme imbalances, and offer promising solutions

based on existing benchmarks [5].

Since real-world industrial datasets available for research are extremely scarce, method evaluation is often conducted using computer or laboratory simulated datasets [7]. For this experiment, an existing synthetic dataset based on existing problems, featuring a non-linear problem and hyper-spherical anomaly distribution, is used to evaluate the detectors [8]. Since the probability distributions are known, an ideal anomaly detector can be created for comparison purposes.

By varying the simulation parameters to create cases where 100% classification is not possible and generating very large testing datasets, the models can be evaluated for their ability to generalize to new data from the same problem. Two distributions were selected, the first with two features and second with ten, which respectively represent easy and difficult cases [8].

Based on considerations specific to industrial problems, specific requirements are formulated for the detectors (Section I-A4), which are used to create the evaluation criteria, the testing scenarios, and select most promising prevailing methods from existing research for testing [5]. Detectors are evaluated for their overall performance

using the area under the receiver-operator curve (AUCROC), false negative rate (FNR) and false positive rate (FPR). Their ability to generalize is measured through the differences in performance metrics between the validation and testing sets. The risk of selecting a poor performing detector based on validation performance is examined. Based on these results, recommendations are made for applications and further research.

To outline, the contributions of this paper are:

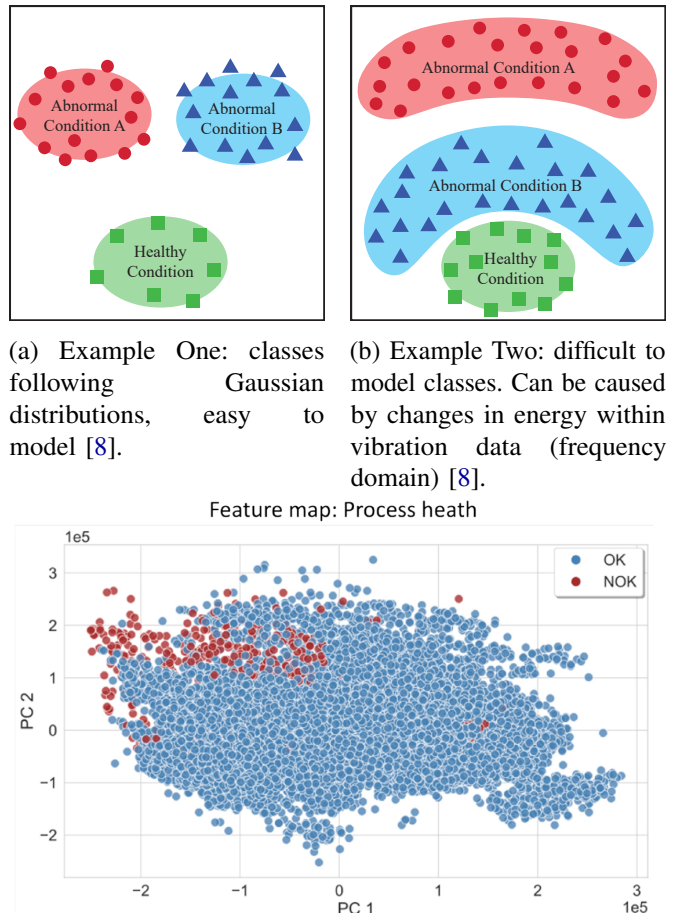
- A comparison of anomaly detection algorithms against themselves and an ideal model, under very imbalanced training conditions.
- Evaluation of the best unsupervised, semi-supervised, and supervised anomaly detectors given different numbers of faulty and healthy examples.
- Investigation of the generalizability of models, based on differences between validation and testing metrics.

A. Industrial Application-Specific Considerations

Based on consultation and literature review, a variety of ongoing challenges in industry have been selected to formulate the basis of the testing scenarios, as they may benefit from anomaly detection techniques. These issues represent specific barriers to machine learning implementation for quality and maintenance purposes in industrial settings. This section takes a closer look at the issues, their possible causes and how they contribute to the requirements.

1) *Class Imbalance*: For many industrial problems, high class imbalance (under 1%) is a significant issue [10], meaning that a very low number of faulty or defective examples may be available for training. Several factors contribute to this issue, including: naturally rarely occurring defects, difficulty/cost in data labelling, and the possibility of novel/unknown anomalies occurring under real-world conditions. While some of these issues may be mitigated by how the system is implemented, or data is collected; in other cases, high class imbalance can be easily corrected.

For example, on a production line, product quality may already be very high at the point that the detection system is to be introduced [9]. Depending on the system and kind of defect to be detected, there may already be existing quality checks that would reduce the number of defective products that make it to the data collection point. This is a particular issue for end-of-line (EOL) testing, as this should be the point in the system with the highest quality levels, thus making it one of the hardest points for collecting data on defects.



(c) Example Three: top two components extracted from principal component analysis applied to CNC milling data [9].

Figure 1: Examples cases of structures seen in research.

Ideally, the data collection would occur on the line as close as possible to where the defects are introduced. However, this is not always possible, or practical. For example, some tests may only work on a completed, or partially completed product. Or, it may not be known at what stage of the production process a defect is introduced.

Additionally, the resources required to perform the tests needed to gather data labels may be prohibitive. Some tests may require skilled labour, specialized equipment, and/or be destructive in nature. By nature, destructive quality tests can only be performed on a small number of products, and are the only option for some applications. These obstacles can make it much more difficult to collect labelled data from a production system.

Another option would be to purposely introduce defects or damage product(s) for the purpose of collecting data. Obviously, intentionally damaging goods is not a preferable option, and cost and waste is not the only issue with this approach. It is vital that the data from the artificial defects match what would be expected

from natural causes. Unfortunately, some defects can be difficult to replicate [7]. While artificial data may still offer benefit for training, as long as the distributions are different, it does not fully substitute real data.

Also, to create a defect for the purposes of data collection, it is assumed that the type (or types) of defect being searched is known. This is a different problem than simply attempting to detect **any** defect, including ones that may not have been previously seen. These are two different approaches, of which the choice depends on other factors: such as, if the system needs to identify if the product has a defect or what the defect is (diagnosis). In this case, we'll assume that we do not have examples of every defect that we want the system to detect. Given that these are cases where such a small number of faulty examples are available, this is a reasonable assumption.

2) *Prior Knowledge*: In this paper, “anomaly” data is typically referenced as a single class, however, many different types of defects may be labeled as anomalous. So, while an individual defect may follow a Gaussian distribution (a combination of its own distribution plus measurement error); as the number of possible defects increases, it becomes less likely that the distribution of the overall anomaly class is Gaussian. Some defects, either naturally or due to feature extraction techniques, follow distributions that are difficult to model, as shown in Figure 1.B.

In such cases, “model-free” or “data-driven” methods, where the underlying physical model of the problem is not known, and where a more general model is tuned using the data itself, are preferable approaches. Generalization issues may occur because the learned model is based on the data, not knowledge of the system; and may overfit to that data, resulting in unexpected deviations in performance on the system, when deployed in the real world. Identifying and correcting for generalization issues is still an ongoing research problem, but it is key that the models perform accurately and consistently on the problems they are trained on.

3) *Ability to Prioritize*: Depending on how a particular quality system is integrated into the production line, the False Positive Rate (FPR) or False Negative Rate (FNR) may be more important than the overall error rate. A false negative on a defective product means it moves onto the next stage, an undesirable result, but the severity of the detection failure is fully dependent on the application. In the case of testing food for dangerous bacteria, a false negative could lead to consumer hospitalization. However, in the case of failing to detect a cosmetic issue, such as a paint bubble, the risk of customer dissatisfaction is much lower. On the opposite side, a high false positive rate may lead to needless waste, expensive downtime, or alarm

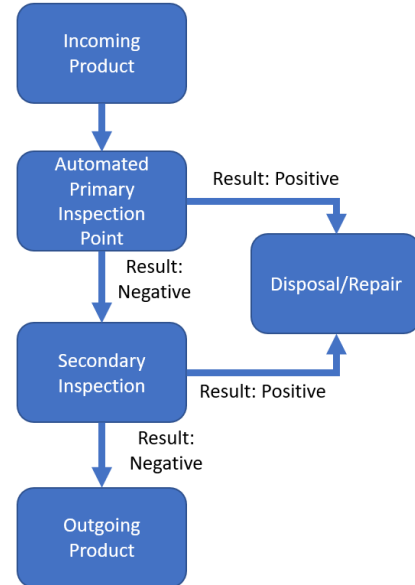


Figure 2: Example where false positives may be prioritized as they result in direct waste, whereas false negatives can be caught by a secondary inspection.

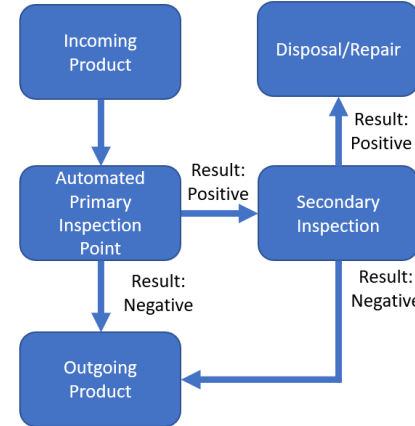


Figure 3: Example where false negatives may be prioritized, as product directly exits system after passing screening.

fatigue (loss of trust in the detection system). Depending on the consequences and severity of false negatives and false positives, different applications may prioritize the cases differently.

On top of that, these quality systems exist as part of a larger production system which may contain multiple testing points. Figures 2 and 3 show examples of two different setups where a single automated quality system may be combined with a second, more accurate quality check. While this does require the use of two systems rather than one, an obvious downside, it can still be useful. For example, the secondary inspection may be worker-operated and the first inspection may be automated, so

Category	Source	Name	Year	Number of Examples	Anomaly Rate
Product Quality	[6]	Bosch Production Line	2016	1,183,747	0.6%
Product Quality	[9]	Bosch CNC Machining	2022	851	4%*
Tool Health	[11]	Blade Wear Sample	2018	6	50%
Tool Health	[11]	Blade Wear One Year	2018	519	N/A
System Monitoring	[12]	Plant Fault Detection	2015	672,530	30%
System Monitoring	[13]	Versatile Production	2018	10,529	N/A
System Monitoring	[14]	Tinsley E-coating	2020	111,361	N/A
Monitoring	[15]	Wind Turbines	2018	40,430	N/A
Monitoring	[16]	APS	2018	60,000	2%
Monitoring	[17]	Hard Drives	2025	452,991,106	1%

Table I: Summary of open-source production datasets [7]. N/A indicates unlabelled data.

* True production rate is reported to be lower.

that the automated system acts as a rapid screening tool and reduces the overall workload.

In any case, the flexibility of being able to prioritize the correct detection of positives over negatives, or vice versa, is a key feature in allowing the detectors to be adapted into multiple use cases. To go even further, the output of an anomaly “score” allows for even more flexibility for applications and decision-making. Because of this, we are going to focus on detection methods that output scores rather than labels.

4) *Summary*: Based on these considerations, the anomaly detection technique should have the following characteristics:

- R.1 Require very low numbers of faulty examples.
- R.2 Produce generalizable results on the problem.
- R.3 Produce consistent results on the problem.
- R.4 Do not require prior information about the problem (data-driven).

Outside of these requirements, there are additional preferential characteristics. There is a preference for more “black box” style methods, with less reliance on low numbers of user-defined parameters. Methods which produce deterministic results (not utilizing random seeds) are more desirable. Given the variety of input data across different applications, consistent performance over different numbers of features is also desirable.

II. BACKGROUND

Previous work benchmarking anomaly detection algorithms for manufacturing has been studied for different applications, including images of products [18], production schedules [1], additive manufacturing [19], sensor data [2] and more. This section will briefly

cover the different types of data-driven algorithms and datasets used for evaluation. Several detectors across these categories are selected for testing, based on previous research (discussed further in Section IV-C).

A. Anomaly Detection Strategies

Anomaly detection algorithms are often categorized by how they use labels: unsupervised, semi-supervised and supervised. Labels indicate if any sample is known to be healthy or faulty (assumed to be binary at this point). Within each of these categories, further categories of algorithms exist (more detailed coverage can be found in [5]).

In unsupervised approaches, no labelling information is required. Methods in this category focus on learning the distribution of the data, thus identifying new data as anomalous when it is “dissimilar” to the training data. These methods are closely related to outlier detection and known to have difficulty detecting clustered anomalies (when present in training data). The absence of class information makes determining a class boundary difficult, so some methods require the user to provide the expected number of faulty examples in the training dataset (the “contamination” rate).

This category comprises the most classical machine learning techniques, such as density estimation (kNN and LOF) and clustering-based methods (CBLOF). It also includes unsupervised adaptations of classification algorithms, such as IForest and OCSVM. A few deep learning (DL) methods (a sub field of multilayer neural network architectures) have also been adapted to unsupervised anomaly detection but continue to struggle with a lack of labels [5].

Supervised approaches require labels for all training data and employ a classification strategy. In cases with a very large class imbalance, class re-weighting can be applied to prevent the classifier from outright favouring the majority class. However, these methods are known to be prone to overfitting with small numbers of examples and/or high numbers of features. They also may not perform well when the anomaly data present in the training dataset is not similar to the anomaly data in the test set (for example, if the fault conditions are different) [5].

Lastly, semi-supervised learning is a combination of unsupervised and supervised learning strategies, which covers a very broad range of strategies; in an attempt to utilize the advantages of both approaches. For example, the use of an unsupervised dimensionality reduction technique with a classifier would fall into this category. For labels, from purely a black-box perspective, semi-supervised methods may require some partial labelling or complete labelling of all training data.

The two main types of semi-supervised anomaly detection algorithms are DL-based, and ensemble-based; which involve combining the results of multiple detectors to improve overall performance. In XGBOD, the output of unsupervised detectors is combined with boosting algorithms to create a semi-supervised detector. Similarly, DL methods have also been developed which combine unsupervised (for example, autoencoders) and supervised techniques (for example, a fully connected neural network).

Semi-supervised methods have shown promise in areas where fully supervised methods struggle [5]. (A review of deep learning strategies for manufacturing by sub-application is covered in [4].) While DL has recently risen in popularity, other methods still make up the majority of algorithms applied to sensor data [2].

Unsupervised and semi-supervised are the most common types of algorithms applied to manufacturing problems. However, research does suggest that semi-supervised methods are best, even when very low numbers of examples are available [5]. There are no guidelines for selecting between unsupervised, semi-supervised or supervised strategies, based on available dataset size outside of specific problems (e.g. images defect detection).

B. Available Datasets

Comparisons of anomaly detection algorithms primarily rely on simulated data (real-world or computer-generated) due to the lack of open-source production datasets [10], [7]. A summary of available production

Class	Distribution Type	Parameters
Healthy	Three-mode	$\sigma_A^2 > 0.01, \mu > 0,$
	Gaussian	$\mu_A = \sqrt{\mu^2/d},$
	Mixture	$\mu_1 = \vec{0},$ $\mu_2 = \mu_A \vec{1},$ $\mu_3 = -\mu_A \vec{1}$
Faulty	Gaussian Mixture	
	Hypersphere Approximation	$r_B = \mu/2,$ $\sigma_B^2 > 0.1$

Table II: Allowed parameters for TvS distribution type [8]. d is the number of features.

datasets is covered in Table I, giving an idea of the large number of examples and low anomaly rates that form the problem. Due to the small number of production datasets, anomaly detectors are often benchmarked with simulated data or other benchmark datasets [5], [10], which have higher anomaly rates. However, many techniques have been applied to control the anomaly rate including:

- Stratified Sampling: Keeping the anomaly rate in the training and testing datasets the same [5].
- Modified Labels: Class labels may be changed to make the problem more difficult [5].
- Downsampling: Reducing the number of examples by removing examples from the dataset [20]. By deleting healthy or anomalous examples, the anomaly rate can be controlled.

These methods do have different underlying effects on the experimental setup. For example, changing some anomaly labels to healthy may reduce the apparent number of anomalous examples in the training dataset [5], but that data is still present and may change the behaviour of anomaly detectors which make use of the labels. Note that any combination of the methods listed above means that the labelled anomaly rate for any dataset may be artificially lowered to under a 1% total anomaly rate. Additionally, the ratios used for train-test splitting do also directly influence the amount of data available for training and the number of anomalous examples.

The low number of anomalous examples in production datasets makes it difficult to properly measure performance. This is one reason why synthetically generated computer datasets have been used for testing detectors. Some synthetic datasets use simulation models based on existing processes [21], but others also use Gaussian distributions and similar clusters [22], [23], [24]. In this case, a subset of the dataset from [8] is used, as it represents a difficult scenario and includes known probability distributions for both faulty and healthy.

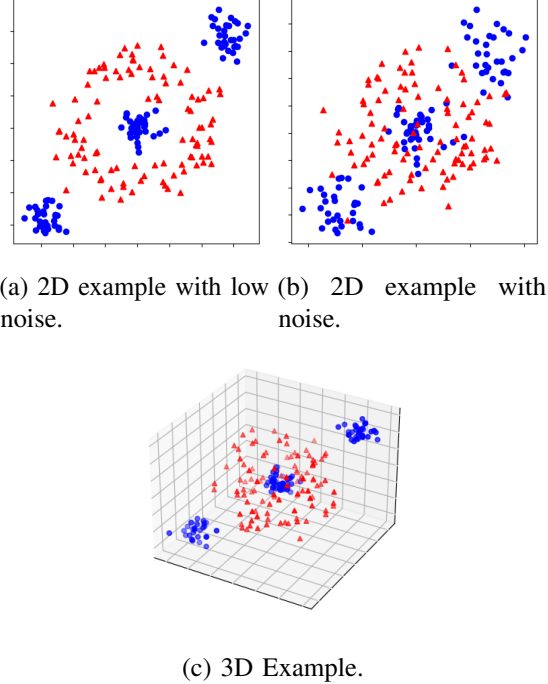


Figure 4: Examples of TvS distribution [8].

C. Simulated Dataset

This experiment will make use of the “TvS” distribution from [8], where the healthy data follows a spaced-out three-mode Gaussian mixture, and the faulty data forms a hypersphere (see Figure 4). This works well as a test case because it produces a scenario where all features contribute to the class separability, the number of features can be controlled and the faulty class is spread out.

Table II covers the distribution parameters. μ controls the offset while σ_A and σ_B control the noise levels for the two classes, as shown in Figure 4. By varying the μ , σ_A and σ_B user-controlled parameters, the overall separability of the two classes can be controlled.

Approximately 200 clusters are used to create the hypersphere approximation, and when a small number of faulty examples are available, this makes it difficult to model the faulty distribution. However, it is not expected that the faulty distribution would be easy to model, predictable, or consistent due to the nature of the faults. Therefore, this is a good test case for our scenario.

This distribution does ensure a case where all features are “useful” and the number of features can be controlled. Even in higher dimensions, the structure of the hypersphere still produces a similar problem, although the difficulty of the problem will naturally increase due to the curse of dimensionality.

Although the features have no contextual meaning, every feature is required in order to obtain the best

classification rates. While the Gaussian nature of the structure and small feature space does most closely match sensor data compared to other forms of input data, this could be considered as a case where the original data has already been transformed. As the original input data may be in the form of signals, images or other types of information, there would be an assumption that proper feature extraction and dimensionality reduction has already been applied. Thus, only the distribution and underlying separability are of concern.

A common concern in anomaly and outlier detection, is what type of anomaly is being searched for. As this is a classification problem, the anomalies are simply examples generated by the anomaly class. However, it means that the anomalies may not fit into typical anomaly categories such as “local” or “global”. Thus, the results of the detectors may not be as predictable.

This dataset also supplies the probability distributions, which allows the calculation of the ideal case. This means that the problem difficulty can be controlled, as in a problem can be created where 100% classification is not possible.

III. GROUND TRUTH CALCULATION

In order to evaluate the performance of the detectors against ideal results, an optimal or “ground truth”(GT) anomaly detector is required. Here, the GT anomaly detector is constructed based on the Bayes Classifier, which can only be used when the class probability distributions are known. Given the probability distribution function for the healthy data is PDF_H and faulty is PDF_F , with data point x , the predicted label by the Bayes Classifier is [25]:

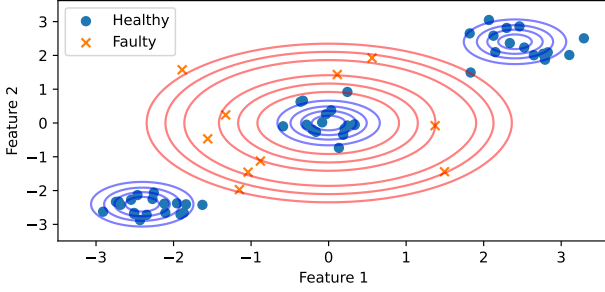
$$\hat{y} = \begin{cases} 1, & \text{if } \text{PDF}_F(x) > \text{PDF}_H(x) \\ 0, & \text{if } \text{PDF}_F(x) < \text{PDF}_H(x). \end{cases} \quad (1)$$

While this classifier has the lowest overall classification error rate on the basis of probability, it does not natively allow for control over the FPR and FNR. In order to obtain finer control over the error rate, Eq. 1 can be turned into a relative anomaly score:

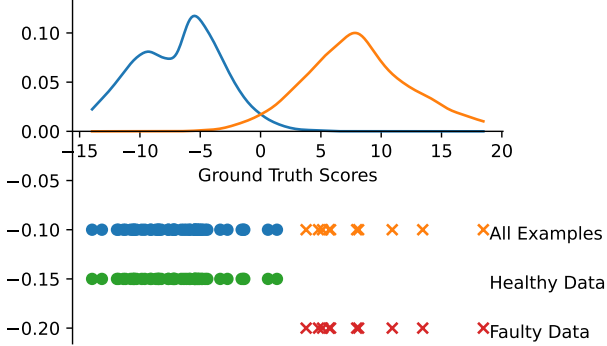
$$g = \log \frac{\text{PDF}_F(x)}{\text{PDF}_H(x)}, \quad (2)$$

$$g = \log[\text{PDF}_F(x)] - \log[\text{PDF}_H(x)]. \quad (3)$$

The ratio is taken here because the probability values can get very small in higher dimensions and the conversion to logarithms can help mitigate the chance of floating point errors. To be consistent with other anomaly detection methods, higher scores indicate a higher likelihood of an anomaly. Figure 5 shows how the TvS distribution



(a) Contour plot of class probability distributions for an 2D example distribution with 50 healthy and 10 anomaly random samples. Parameters: $\mu = 1.8$, $\sigma_A^2 = 0.1$ and $\sigma_B^2 = 0.06$ (see Table II for parameter explanation).



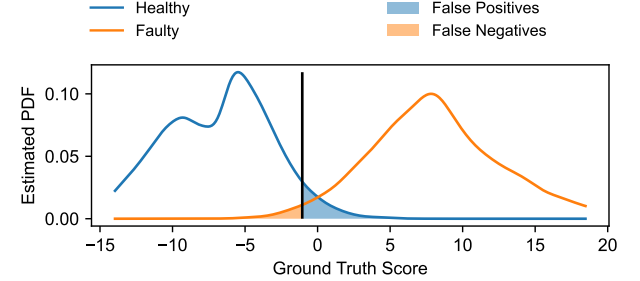
(b) Kernel Density Estimate constructed based on 10000 samples of each class from distribution (a). Scores of samples shown in (a) are included below the graph.

Figure 5: Example of class distributions and scoring distributions for one TvS scenario.

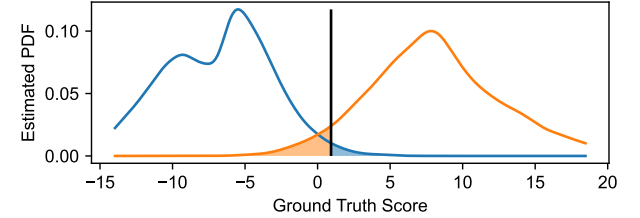
may be used to produce anomaly scores. While this does provide us with an ideal scoring function, those values must still be converted into labels for the purpose of calculating error rates.

A. Simple Anomaly Predictor

In order to convert the anomaly scores g into a classification model to calculate error rates, a threshold must be set to decide how to classify new points. A simple way to do this is to set the threshold based on the empirical inverse cumulative distribution function (percentile/quantile function) for one class based on the available data and target error rate. From that threshold, the error rate from the opposite class can then be estimated from its own empirical cumulative distribution function (see Figure 6). By repeating this process for a range of target percentiles for both classes, an approximate curve of the FPR-FNR trade off can be constructed (see Figure 7).



(a) False positive target rate of 5.00% with a FNR of 1.69%.



(b) False negative target rate of 5.00% with a FPR of 1.42%.

Figure 6: Examples of target error rates for distribution in Figure 5. Estimated PDF is created using kernel density estimation.

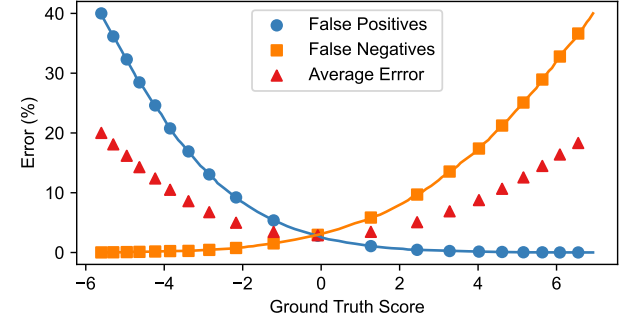


Figure 7: Trade off between false positives and false negatives based on different thresholds for the distribution in Figure 5.

To calculate the estimated FNR (\widehat{FNR}) from a target FPR (FPR_T) using estimates of the CDF and ICDF from the anomaly scores of the healthy and faulty datasets:

$$\hat{t} = \widehat{ICDF}_H(1 - FPR_T), \quad (4)$$

$$\widehat{FNR} = \widehat{CDF}_F(\hat{t}), \quad (5)$$

where \hat{t} represents the estimated threshold.

The threshold \hat{t} can be used as a decision boundary to convert any scoring function into a prediction function. This method also be used on the scores obtained from other anomaly detectors (see Section IV-B).

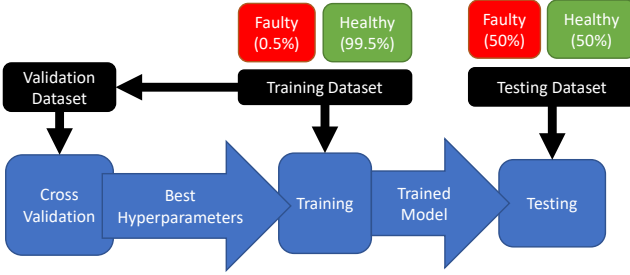


Figure 8: Model training and testing process.

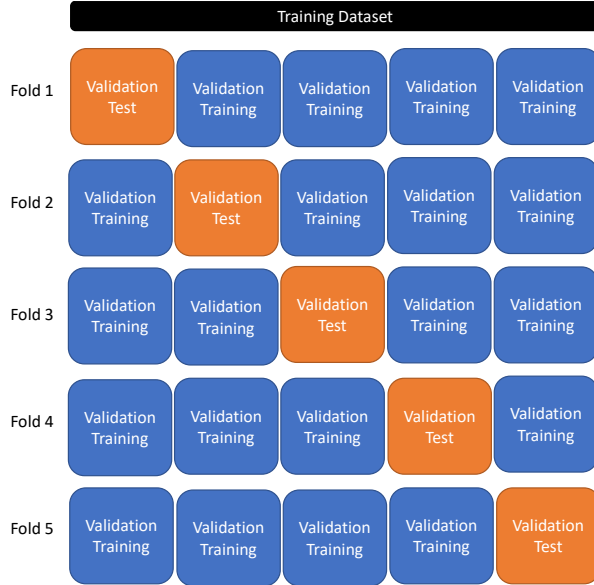


Figure 9: Visual diagram of splitting training dataset for validation.

IV. EXPERIMENT

Each simulation begins by generating the training dataset based on the distribution parameters (Section IV-A) and simulation parameters (Table III). The anomaly rate for the training dataset is set to 0.5%, which represents a very high class imbalance. Small deviations are introduced in the number of training examples (Table III) to introduce some variability. A different preset seed is used for every simulation to ensure reproducibility.

Once the training dataset is created, the validation datasets are created. These datasets are used for calculating validation metrics (Section IV-B) and hyperparameter tuning (see Section IV-D). Each detector has access to the same validation datasets.

Next, the detectors are retrained using the entire training dataset and applied to the testing dataset (see Figure 8). The detectors are given access to all the training data (and labels) to give them the best chance of success at the problem, as would be done in deployment. In this case, all the training data represents what is available and

Basic Simulation Parameters	Values
Target FPR	1%
Number of Training Samples	$1000 \pm 2, 2000 \pm 2, 5000 \pm 2, 10000 \pm 2$
Faulty Rate in Training Samples	0.5%*
Number of Testing Samples	40960†
Faulty Rate in Testing Samples	50%
Number of Simulations	
per Sample Size	100
per Distribution Scenario	

Table III: Simulation Parameters.

* Further examination includes rates of 0.05% to 20%.

† Composed of 40 batches of 1024.

Scenario	Distribution Parameters	Ground Truth Metrics
S_1	$d = 2, \mu = 2.8, \sigma_A^2 = 0.05, \sigma_B^2 = 0.4$	FPR = 1.0%, FNR = 7.4%, AUCROC = 99%
S_2	$d = 10, \mu = 1.05, \sigma_A^2 = 0.02, \sigma_B^2 = 0.04$	FPR = 1.0%, FNR = 15%, AUCROC = 99%

Table IV: Synthetic dataset simulation parameters for TvS data generation (variables are covered in Table II) and associated ground truth metrics.

the testing data represents the world.

A. Test Cases

Using the TvS distribution (Section II-C), two specific test cases were selected, named S_1 and S_2 , with 2 and 10 features respectively (details of the distribution parameters are covered in Table II). Based on the results of [8], the TvS distribution was a very difficult case when used with 8 and more features, thus the 10 feature case (S_2) is also expected to be a challenge for the detectors.

Given that the simulated dataset does not have a limit to the number of examples that can be generated, Monte Carlo simulation can be used to approximate the ideal performance metrics for a distribution (Section III). In this case, 10 240 batches of 1024, for a total of 10 485 760 points for each scenario, are used to calculate the ground truth in Table IV.

The distribution parameters (Table II) were purposefully chosen to create a problem where the ideal AUCROC scores are similar and the classes are not fully separable. This was done for two reasons: to create a more difficult problem and to more easily identify cases in which detector performance is overestimated. While the ideal error rate is not low enough to be acceptable for many applications, using a harder problem is better for

evaluating detectors. This problem is separable enough, so that it may easily “appear” to be fully separable in the training dataset, even though it is not.

Remember that the overall separability of the problem is not known in practice, although it is typically assumed that the problems are “solvable” with the available data and a 0% error rate is achievable. Here, a different approach is taken, given that it is known that there will be a trade-off between the FPR and the FNR. In this experiment, the target or desired FPR is set to 1% and the goal is to capture as many faulty examples as possible while maintaining that FPR. In effect, a 1% FPR is considered to be “acceptable” for these problems (which may vary in practice). It is important to note that setting the target error rate based on FPR is much more reliable than FNR due to the small number of faulty examples available for training.

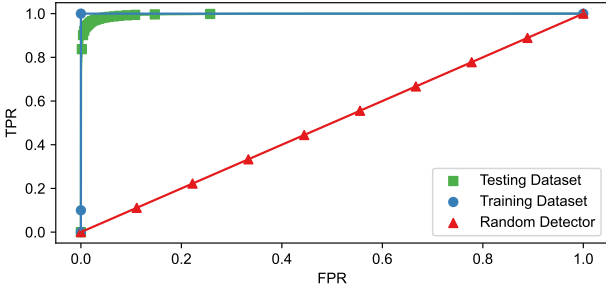


Figure 10: Example ROC curves for ideal cases in Figure 7 and random case.

B. Metrics

As the anomaly scores for each detector are relative and can not be directly compared, the base metrics used to measure detector performance in each simulation are:

- AUCROC: Area Under the Receiver Operating Characteristic Curve
- FPR: False Positive Rate
- FNR: False Negative Rate

The Receiver Operating Characteristic Curve shows the rate of true positives against false positives across all threshold settings (Figure 10) and the AUCROC is the area under the curve. Given sets of faulty and healthy data ($X^{(f)}$ and $X^{(h)}$) with n_f and n_h points, respectively, the AUCROC is calculated as:

$$\text{AUCROC} = \frac{\sum_{i=1}^{n_f} \sum_{j=1}^{n_h} \mathbf{I}(s(x_i^{(f)}) > s(x_j^{(h)}))}{n_f \cdot n_h} \quad (6)$$

where I is the indicator function and $s(x)$ corresponds to the raw anomaly detection score of point x for each detector. Given that the problem is already binary, no

modification is needed, class imbalance is already taken into account.

AUCROC is a very common metric for evaluating anomaly detectors [10] because it condenses the trade-off between false positives and false negatives into a single metric (Figure 7). However, this means that any AUCROC value may correspond to multiple different curves with different behaviors (for example, as in Table IV).

Therefore, in addition, the simple anomaly predictor from Section III-A is also applied to the anomaly detection scores to produce labels from the anomaly scores. Thus, detector performance at the target FPR can be compared, as well as consistency on the test set. While some detectors already have their own prediction functions, using a single method for this step removes inconsistencies in different implementations.

Note that since the CDF and ICDF functions used in Equations 4 and 5 are estimates, constructed empirically based on the available scores, their accuracy is also influenced by the number of examples. Small sample size may cause variation in the interpolation results and jumping.

C. Detectors

Based on the problem criteria (Section I-A), existing detectors were sought out that had been previously evaluated and performed well on datasets with very small numbers of anomalous examples. Based on the results of [5], the detectors were selected based on high average AUCROC scores on a large number of benchmark datasets, when only trained with 1% of the dataset’s anomalies being labelled. Given that unlabelled anomalies still existed in the training datasets, this case is slightly different, however, the small number of labels means the problem was still difficult.

Pre-scaling is integrated into every detector (other than ground truth), so that the input is scaled to unit variance and zero mean. The selected detectors are listed in Table V. Unless listed in Table V, hyperparameters were left at the default values of [5]. The implementation of the detectors is kept as close as possible to the versions used in [5], with some exceptions for unsupervised methods.

1) *Modifications to Unsupervised Methods:* Note that in this application, there is an assumption that the labels are available, but the purpose of this experiment is **not** to examine the benefits of using labelled vs. unlabelled data. Thus, unsupervised detectors face a natural disadvantage (not utilizing labels) over supervised detectors.

There are known issues which can occur when giving anomalous data to the unsupervised detectors. For

Category	Type	Set Hyperparameters and Value	Tuned Hyperparameters and Allowed Values
One-Class Unsupervised (US)	CBLOF	None	n_clusters: 4, 6, 8, 10, 12
	DeepSVDD	None	None
	IForest*	contamination: 0.01	random_state: 0 to 49 n_estimators: 50, 75, 100 max_samples: 'auto', 0.5, 0.7, 0.8, 0.9
	kNN	contamination: 0.01	n_neighbors: 3, 5, 7, 0.001N, 0.01N, 0.02N, 0.03N, 0.04N, 0.06N, 0.08N, 0.10N, 0.12N, 0.15N †
	LOF	contamination: 0.01	n_neighbors: 3, 5, 7, 0.001N, 0.01N, 0.02N, 0.03N, 0.04N, 0.06N, 0.08N, 0.10N, 0.12N, 0.15N †
	OCSVM	contamination: 0.01	kernel: sigmoid, rbf, linear gamma: auto, scale nu: 0.3, 0.5, 0.7, 0.9
	DeepSAD	None	seed: 1, 2, 3, 4, 5
Two-Class Semi-supervised (SS)	DevNet	None	seed: 1, 2, 3, 4, 5
	PreNet	None	seed: 1, 2, 3, 4, 5
	XGBOD	None	random_state: 1, 2, 3, 4, 5
	CatBoost	None	None
Two-Class Fully Supervised (FS)	FTTransformer	None	seed: 1, 2, 3, 4, 5
	SVM	class_weight: balanced break_ties: True	kernel: sigmoid, rbf, linear gamma: auto, scale c: 0.1, 0.3, 0.5, 0.7, 1.0, 1.2, 1.5, 1.7, 2.0
	XGB	None	None

Table V: Custom anomaly detector parameters. In cases where it is None, no hyperparameter tuning was done and default parameters were used. System specific and debug parameters (memory allocation, GPU selection, verbosity, etc.) are excluded.

* Indicates that only certain combinations were used.

† N is the total number of training samples. Fractions are rounded up.

example, if anomalous points start to form clusters, then kNN will start to recognize them as part of the distribution rather than anomalies. Depending on the type of anomaly, this data may influence the detector in unexpected ways. Thus, the unsupervised detectors are treated in this case as “one-class” detectors, by removing the anomalous data from all training datasets.

Due to this, and how the labels are also used in cross-validation; and inform hyperparameter selection, the “unsupervised” detectors are not truly unsupervised. This terminology is simply to represent the different approaches used by the detection methods.

D. Hyperparameter Selection and Validation

For hyperparameter selection, five-fold cross validation is used, meaning the training dataset is split into five train-test subsets (See Figure 9). In each case, the model is trained on four of the subsets (80%) while one is

reversed for testing (20%). Faulty examples are evenly divided (or as closely as possible) between each subset. Note that this requires a minimum number of five faulty examples in the original training dataset.

The validation metrics are taken as the average values over the five testing datasets. For models with hyperparameter tuning (Table V), those values are selected based on the highest validation AUCROC. This cross-validation step is performed even for detectors with no hyperparameter tuning to obtain validation metrics. The validation metrics serve as predictors of model performance on the testing dataset and will be used later on for checking generalizability.

For detectors that use random initial seeds values, those seeds are included as parameters to be tuned. For LOF and kNN, the number of neighbors used is expanded beyond the list used by [5] to include ratios based on the total numbers of training examples. While the ideal hyperparameters for these detectors are known to vary,

based on the number of examples [26], and this change may not fully correct for that variation, the 80% training validation size vs. a 100% training dataset size difference, is not expected to be large enough to cause issues.

E. Implementation

The program used to conduct the simulations is provided at github.com/LesleyWheat/AD-imbalanceTester. For the sake of reproducibility, only anomaly detection techniques with open-source implementations were applied (Table V). Although there may be some variations from computation on different hardware (for example, CPU vs. GPU), this is expected to be negligible in the overall results.

All detection methods must complete successfully in order for a simulation to be counted. During hyperparameter tuning, values which result in errors are excluded. In the case where no valid hyperparameters are found, or the chosen hyperparameters produce an error when the method is applied to the full training dataset, the simulation is excluded from the results.

V. RESULTS

A. Test Performance

The overall ranks from the simulation testing AUCROC results are reported in Figure 11 to compare against the results in [5]. In the critical difference diagram, the datasets sizes are all combined, and show kNN and LOF as the top detectors. However, this picture does not tell the entire story, and from the expanded results in Table VI, the ranking of the detectors is highly dependent on the total dataset size.

Looking at the performance for different training dataset sizes, the top detectors on the S_1 case are kNN, LOF and SVM. For the smaller training datasets, kNN

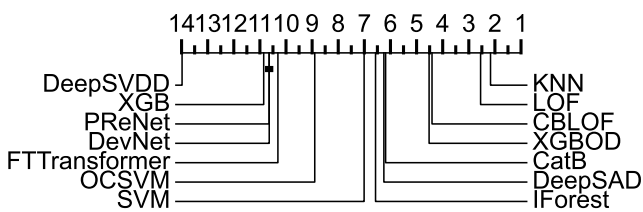
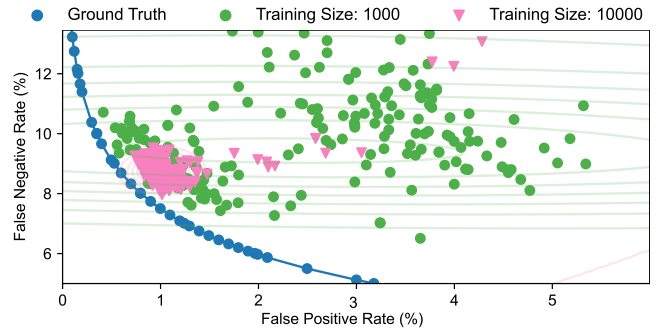
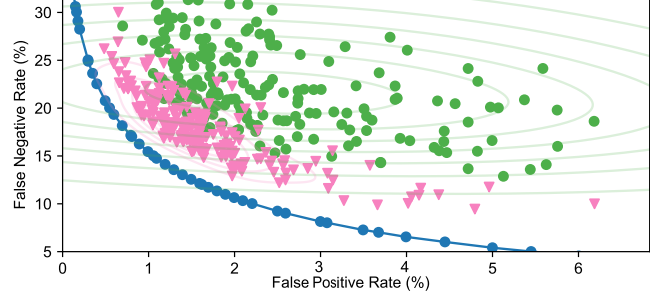


Figure 11: Critical difference diagram over average rank results over all simulations with a training anomaly rate of 0.5% (minimum 199 simulation per sample size). Results not statistically significant are connected by a black bar. Created using the same method as [5].



(a) Simulation test error rates of LOF on S_1 .



(b) Simulation test error rates of XGBOD on S_2 .

Figure 12: Examples of detector performance differences based on the training dataset size at an anomaly rate of 0.5%. Each point represents the results of a single simulation while contour plots are estimates of the distributions for each set (constructed using kernel density estimation).

is the best detector but as the size increases, SVM performance increases. In S_2 , kNN is also the best detector for small datasets but XGBOD ranks at the top for larger datasets.

Most detectors had decreased performance on S_2 compared to S_1 , as expected due to the increased difficulty of the problem. Additionally, the AUCROC ranges tend to also be larger, reflecting increased performance variability. Interestingly, OCSVM does perform better with more features.

Figure 12 displays the raw results for LOF and XGBOD, illustrating how detectors approach the performance of the ground truth detector with more examples; but tend to have variation in both the false positive and false negative rate. It can also be noted, that the results tend to follow a similar curve to the ground truth, as expected. This also indicates that the false positive and negative rates do not follow a Gaussian distribution.

To look more broadly at the performance over the different types of approaches, in both cases, unsupervised methods comprise the top detectors on the smaller datasets (Table VI). As more examples are added, the

		Number of Training Examples			
		1000	2000	5000	10000
True	TD	(98.9, 99.1)	(98.9, 99.1)	(98.9, 99.1)	(98.9, 99.1)
US	CBLOF	(2.2) (97.1, 98.1)	(4.4) (97.0, 98.1)	(6.7) (96.9, 98.0)	(8.2) (96.7, 98.0)
	DeepSVDD	(13.9) (34.8, 47.3)	(14.0) (39.9, 46.9)	(14.0) (42.1, 46.3)	(14.0) (44.7, 46.3)
	IForest	(3.6) (96.4, 97.9)	(4.3) (97.3, 98.2)	(5.2) (97.7, 98.2)	(5.6) (97.8, 98.2)
	KNN	(2.4) (97.4, 98.4)	(1.7) (97.9, 98.5)	(2.3) (98.0, 98.5)	(3.0) (98.1, 98.5)
	LOF	(3.9) (94.2, 98.5)	(2.1) (95.8, 98.5)	(3.0) (95.6, 98.5)	(3.3) (96.4, 98.5)
SS	OCSVM	(11.2) (47.9, 84.4)	(12.6) (50.5, 84.1)	(13.0) (82.8, 83.8)	(13.0) (82.8, 83.8)
	DeepSAD	(6.3) (92.3, 97.1)	(5.9) (94.5, 98.4)	(5.7) (95.5, 98.5)	(6.4) (96.2, 98.5)
	DevNet	(9.3) (53.0, 94.5)	(10.1) (83.8, 95.1)	(11.3) (91.2, 95.6)	(11.6) (92.9, 95.5)
	PReNet	(9.3) (52.7, 94.4)	(9.6) (81.5, 95.0)	(10.9) (92.8, 95.4)	(11.3) (94.0, 95.6)
	XGBOD	(4.4) (95.3, 98.2)	(5.5) (95.2, 98.3)	(6.1) (96.4, 98.4)	(5.9) (96.8, 98.5)
FS	CatB	(6.3) (80.2, 98.0)	(5.9) (87.3, 98.3)	(4.2) (96.8, 98.6)	(3.0) (97.7, 98.7)
	FTTTransformer	(8.6) (71.5, 97.3)	(9.1) (82.8, 97.5)	(10.1) (91.4, 97.7)	(9.0) (94.0, 98.2)
	SVM	(11.9) (15.5, 94.8)	(9.0) (50.0, 98.5)	(3.6) (93.6, 98.7)	(2.1) (97.6, 98.7)
	XGB	(11.7) (51.2, 86.9)	(10.9) (76.2, 95.1)	(8.9) (93.0, 97.5)	(8.6) (96.2, 97.9)

(a) Results for S_1 (2 features).

		Number of Training Examples			
		1000	2000	5000	10000
True	TD	(99.0, 99.1)	(99.0, 99.1)	(99.0, 99.1)	(99.0, 99.1)
US	CBLOF	(2.3) (95.3, 96.9)	(3.2) (95.2, 96.8)	(4.1) (95.0, 96.7)	(4.0) (96.4, 97.6)
	DeepSVDD	(13.9) (39.7, 50.8)	(14.0) (42.1, 50.8)	(14.0) (46.5, 50.3)	(14.0) (46.7, 50.2)
	IForest	(7.1) (85.8, 93.2)	(7.5) (89.5, 94.5)	(8.7) (91.2, 94.6)	(10.7) (91.7, 95.1)
	KNN	(1.9) (95.4, 97.5)	(1.6) (96.5, 97.5)	(1.9) (96.8, 97.4)	(2.7) (96.9, 97.4)
	LOF	(2.3) (94.0, 97.6)	(1.7) (95.0, 97.6)	(1.8) (96.0, 97.5)	(2.5) (96.7, 97.5)
SS	OCSVM	(4.1) (94.6, 95.7)	(4.5) (94.8, 95.6)	(5.7) (95.0, 95.6)	(7.4) (95.0, 95.5)
	DeepSAD	(7.9) (84.5, 91.7)	(6.1) (91.9, 94.7)	(5.9) (94.0, 96.0)	(5.9) (95.2, 96.7)
	DevNet	(11.0) (65.4, 84.5)	(11.0) (74.3, 89.8)	(10.2) (88.2, 93.4)	(10.7) (91.8, 94.7)
	PReNet	(11.0) (65.5, 83.8)	(11.1) (77.9, 87.9)	(11.1) (86.5, 93.4)	(10.8) (91.5, 95.0)
	XGBOD	(5.3) (87.0, 96.3)	(4.6) (88.5, 97.1)	(2.8) (94.7, 97.7)	(1.5) (96.7, 98.1)
FS	CatB	(5.8) (88.4, 95.2)	(7.9) (88.3, 93.9)	(8.8) (90.2, 94.6)	(7.4) (93.9, 96.5)
	FTTTransformer	(9.4) (68.8, 88.9)	(10.8) (70.2, 89.5)	(12.7) (78.1, 92.1)	(12.7) (85.4, 94.1)
	SVM	(10.4) (35.5, 92.2)	(8.2) (51.4, 95.1)	(6.1) (91.7, 96.7)	(4.8) (94.8, 97.5)
	XGB	(12.7) (47.7, 74.4)	(12.7) (66.0, 84.9)	(11.2) (86.4, 92.9)	(9.9) (92.3, 95.0)

(b) Results for S_2 (10 features).

Table VI: Testing bounds for AUCROC, shown in percent, for simulations with a training dataset anomaly rate of 0.5% (minimum of 199 simulations per sample size). The first bracket contains the average rank by test AUCROC (lower is better) (excluding true detector). The second bracket contains the lower (2.5%) and upper (97.5%) bounds. The top three detectors (excluding true detector), by average rank for each number of training samples, are in bold.

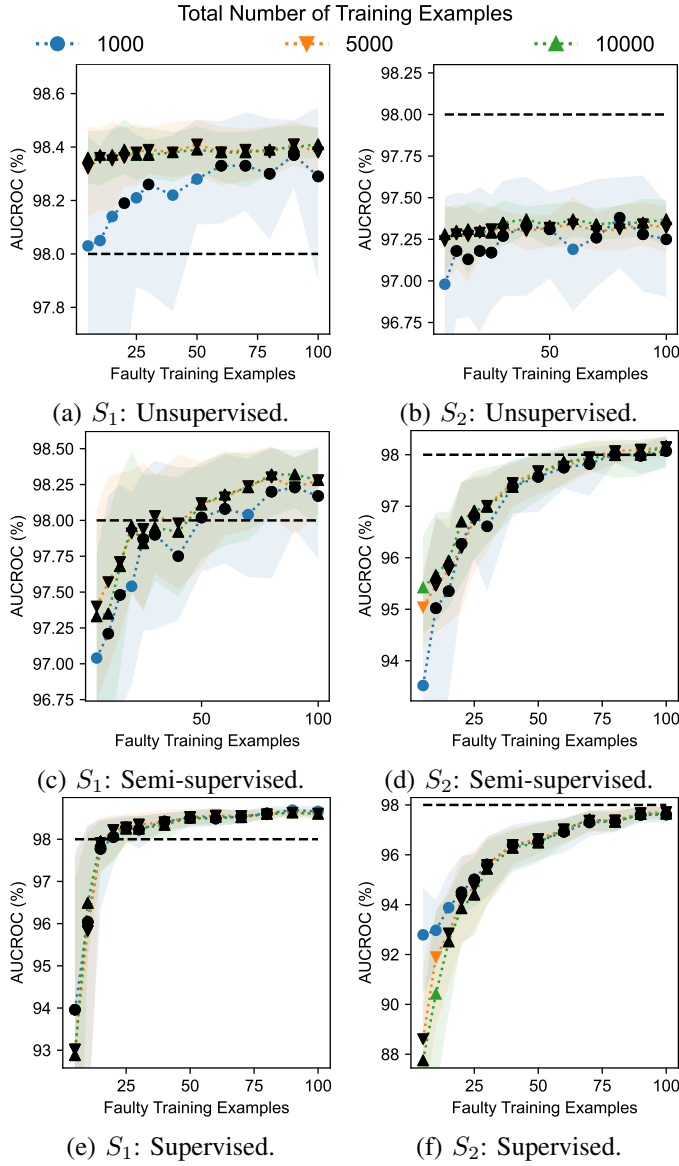


Figure 13: AUCROC by category, for differing numbers of anomalous samples in the training dataset and the training dataset size. Filled areas represent the 80% range (10% to 90% percentile). Icons represent the average for each set of simulations (minimum of 25 simulations) and black icons indicate results that are not statistically significantly different from all other dataset sizes ($p > 0.05$). The black dashed line is at 98% AUCROC for reference.

performance of the top unsupervised methods do not increase significantly, but methods which utilize labels quickly improve as more examples are added. The change in rank is not due to a decrease in unsupervised detector performance, but rather an increase in semi-supervised and supervised detector performance. As well, in the larger feature space (S_2), semi-supervised methods do tend to perform better than the supervised methods.

From the results in Table VI, it is not possible to

Number of Anomaly Training Examples	Total Number of Training Examples		
	1000	5000	10000
5	US	US	US
10	US	US	US
15	US	US	US
20	US	US	US
25	FS	US	US
30	US	US	US
40	FS	FS	US
50	FS	FS	FS
60	FS	FS	FS
70	FS	FS	FS
80	FS	FS	FS

(a) Results for S_1 (2 features).

Number of Anomaly Training Examples	Total Number of Training Examples		
	1000	5000	10000
5	US	US	US
10	US	US	US
15	US	US	US
20	US	US	US
25	US	US	US
30	US	US	US
40	SS	SS	SS
50	SS	SS	SS
60	SS	SS	SS
70	SS	SS	SS
80	SS	SS	SS

(b) Results for S_2 (10 features).

Table VII: Best detection strategy by average maximum AUCROC by number of anomaly examples and total number of training examples (minimum of 25 simulations). Categories from Table V. Bold indicates the results are not statistically significantly different from all other methods ($p > 0.05$).

know if the change in detector performance is due to the increase in faulty examples, or in healthy examples in the training dataset. To examine the impact of adding more of each type of class to the training dataset, more simulations are conducted with differing anomaly rates, to create the results in Figure 13. To simplify the information, the detectors are grouped into categories (as detailed in Table V) and, for each simulation, the maximum AUCROC,

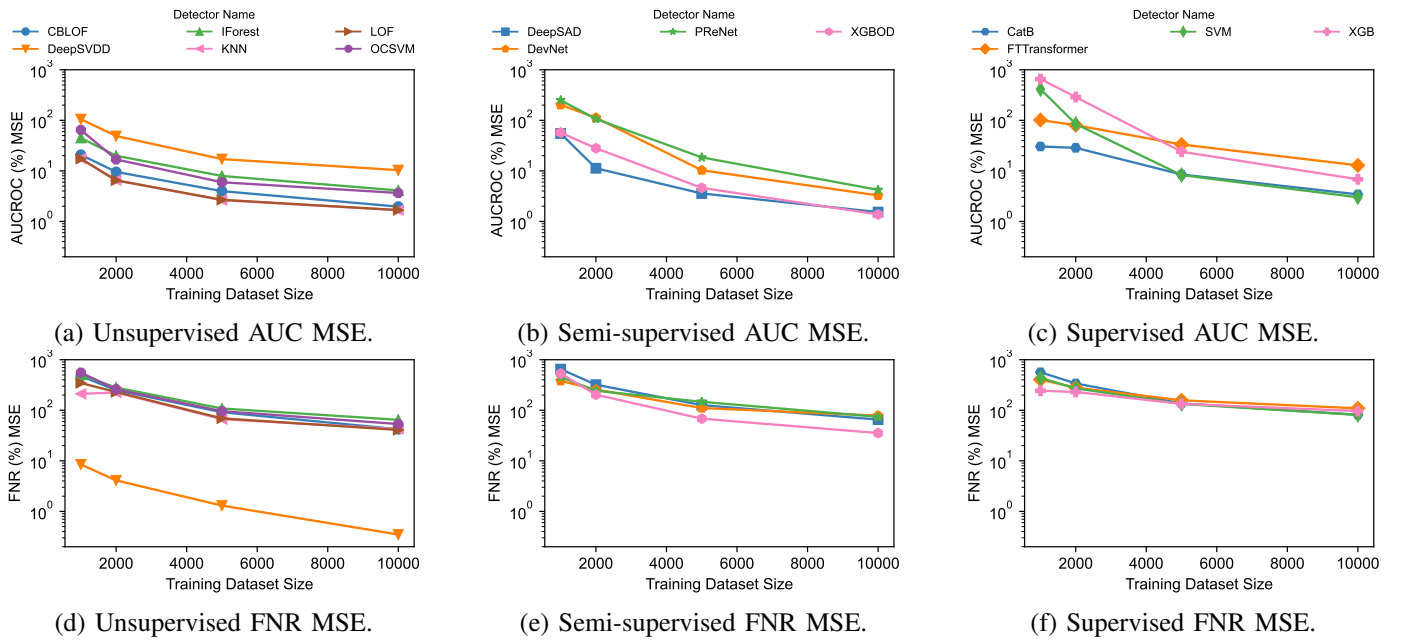


Figure 14: Generalization results of S_2 with a training anomaly rate of 0.5% for different training dataset sizes (minimum of 199 simulations per sample size).

over all detectors in that category, is taken as the category metric.

With 50 simulations per combination of dataset size and number of faulty examples, the results across different numbers of healthy examples are rarely statistically significant (at $p \leq 0.05$). Most statistically significant results are from the smallest dataset (1 000 examples) and where, as expected, the unsupervised methods struggle. Overall, the impact of additional healthy examples to the training dataset is low.

The curves in Figure 13 do have the same general shape as the results reported by [5]. While the results of [5] show most semi-supervised algorithms outperform the best unsupervised methods at 1% labelled anomaly rate, these results show that behaviour only occurs when a minimum amount of labelled faulty examples are available. In [5], the 1% labelled anomaly rate corresponds to different numbers of total labelled anomalies in the training dataset, due to different dataset sizes and base anomaly rates. Here, it is shown that the change in performance is primarily due to the total number of faulty examples in training. These curves are extended on the left side, showing where supervised methods significantly suffer and unsupervised methods have the highest performance.

Based on these results, the best detection strategy is largely determined by the total number of anomaly examples available for training. This is further explored by Table VII, which shows the detection category with the highest average maximum AUCROC for each dataset makeup. From this table, it is clear that unless there are

at least 20-50 anomaly examples available for training, unsupervised methods are the best option.

While the transition from unsupervised occurs at about the same number of faulty examples for S_1 and S_2 , that is where the similarities end. For S_1 , it is better to transition directly to a supervised approach rather than using semi-supervised learning. But in S_2 , it is the opposite, where semi-supervised methods perform better than supervised in all tested cases. Thus, it is apparent that semi-supervised methods have an advantage over supervised methods in larger feature spaces.

B. Generalization

Given that the testing dataset would not be available in a real-world case for detector evaluation, conclusions about detector performance would be drawn from the validation metrics. To examine the consistency and reliability of the detector results, this section will examine the differences in results between the validation and testing metrics.

Firstly, it is worthwhile to look at changes across different performance metrics. Figure 14 compares the MSE of AUCROC and FNR across the different detection methods. In this case, the validation metric can be seen as a predictor variable for the test result. When both measures are taken in percentage, AUCROC is much more consistent for most detectors. Therefore, AUCROC will be used for comparison purposes.

Table VIII shows the error range when using the validation AUCROC to predict testing AUCROC. As an

		Number of Training Examples				
		1000	2000	5000	10000	
Anomaly Detection Method	True	TD	(-1.1, 4.7)	(-1.1, 4.8)	(-1.0, 2.6)	(-1.0, 1.9)
	CBLOF		(3.6) (-2.9, 10.0)	(6.1) (-2.8, 6.1)	(7.6) (-2.8, 3.6)	(8.2) (-2.5, 2.6)
	DeepSVDD		(7.8) (-15.5, 12.5)	(8.6) (-13.1, 9.6)	(9.0) (-6.9, 6.6)	(10.1) (-4.9, 4.3)
	IForest		(3.6) (-3.0, 7.1)	(4.7) (-2.3, 6.0)	(6.3) (-1.9, 4.2)	(6.8) (-1.7, 2.5)
	KNN		(3.9) (-2.6, 6.7)	(3.9) (-1.8, 6.9)	(5.6) (-1.7, 3.7)	(6.3) (-1.5, 2.5)
	LOF		(5.1) (-4.7, 6.3)	(4.1) (-2.8, 5.3)	(5.9) (-3.7, 3.1)	(6.2) (-2.2, 2.2)
	OCSVM		(10.0) (-48.2, 16.8)	(10.2) (-25.2, 13.8)	(11.2) (-10.6, 10.7)	(11.0) (-7.1, 9.4)
	DeepSAD		(6.2) (-7.5, 8.0)	(6.4) (-4.6, 4.5)	(6.4) (-2.7, 4.1)	(6.5) (-2.2, 2.1)
	DevNet		(9.4) (-45.2, 33.0)	(8.3) (-8.1, 13.8)	(8.1) (-4.3, 4.3)	(7.8) (-2.8, 3.4)
	PReNet		(9.9) (-44.0, 32.6)	(8.6) (-9.7, 14.6)	(8.2) (-4.3, 5.9)	(7.9) (-2.8, 3.5)
FS	XGBOD		(6.0) (-4.4, 11.4)	(7.9) (-4.7, 8.9)	(7.2) (-3.5, 3.8)	(7.0) (-2.4, 2.6)
	CatB		(7.8) (-19.1, 17.2)	(6.4) (-9.6, 10.5)	(5.4) (-1.8, 4.1)	(5.3) (-1.3, 2.6)
	FTTransformer		(8.7) (-26.1, 20.6)	(9.1) (-13.1, 10.4)	(9.7) (-7.0, 4.2)	(8.7) (-4.1, 3.8)
	SVM		(11.7) (-54.7, 21.8)	(10.5) (-37.2, 17.6)	(5.6) (-3.3, 8.0)	(4.7) (-1.4, 2.2)
	XGB		(11.1) (-39.0, 55.0)	(10.2) (-17.0, 25.7)	(8.6) (-4.1, 8.1)	(8.5) (-2.4, 4.2)

(a) Results for S_1 (2 features).

		Number of Training Examples				
		1000	2000	5000	10000	
Anomaly Detection Method	True	TD	(-1.0, 5.8)	(-1.0, 2.9)	(-0.8, 1.5)	(-0.7, 1.0)
	CBLOF		(4.2) (-4.3, 12.5)	(5.3) (-4.0, 7.3)	(6.3) (-3.3, 3.6)	(6.4) (-2.1, 3.0)
	DeepSVDD		(8.3) (-22.8, 11.0)	(8.8) (-15.2, 8.6)	(9.4) (-9.6, 5.5)	(9.8) (-7.3, 4.6)
	IForest		(7.5) (-12.3, 10.9)	(7.6) (-7.9, 5.9)	(8.2) (-5.5, 4.0)	(8.6) (-3.8, 4.0)
	KNN		(4.0) (-4.4, 12.2)	(3.9) (-3.0, 6.8)	(5.0) (-2.4, 3.6)	(5.8) (-1.8, 3.0)
	LOF		(3.9) (-5.5, 9.5)	(3.7) (-2.9, 7.3)	(5.0) (-2.3, 3.6)	(5.8) (-1.8, 3.1)
	OCSVM		(5.9) (-5.0, 16.2)	(6.4) (-4.6, 9.6)	(6.9) (-3.6, 5.5)	(8.1) (-2.6, 5.6)
	DeepSAD		(8.0) (-13.2, 5.5)	(6.0) (-6.1, 3.7)	(6.2) (-3.3, 1.6)	(6.3) (-2.4, 2.2)
	DevNet		(10.1) (-25.6, 27.0)	(9.7) (-18.1, 21.1)	(8.0) (-6.1, 6.0)	(7.5) (-3.5, 3.5)
	PReNet		(10.4) (-29.6, 29.1)	(10.0) (-17.9, 22.8)	(9.2) (-8.1, 8.6)	(8.2) (-4.4, 3.9)
FS	XGBOD		(7.5) (-12.0, 15.4)	(7.0) (-11.1, 10.3)	(6.6) (-4.1, 4.2)	(5.4) (-2.1, 2.3)
	CatB		(5.9) (-8.0, 12.2)	(7.5) (-7.5, 11.2)	(7.5) (-4.0, 6.8)	(7.1) (-2.4, 4.8)
	FTTransformer		(8.2) (-22.8, 12.0)	(9.2) (-20.8, 9.6)	(10.0) (-14.2, 5.2)	(10.4) (-7.5, 4.1)
	SVM		(10.2) (-46.9, 18.6)	(8.3) (-20.3, 18.0)	(7.2) (-3.9, 6.8)	(7.0) (-2.1, 4.1)
	XGB		(10.9) (-31.4, 59.0)	(11.6) (-22.4, 35.4)	(9.5) (-5.9, 12.2)	(8.7) (-3.7, 5.8)

(b) Results for S_2 (10 features).

Table VIII: Using validation AUCROC to predict testing AUCROC with a training anomaly rate is 0.5% (minimum of 199 simulations per sample size). The first bracket contains the average rank by lowest squared error (excluding true detector). The second bracket contains the lower (2.5%) and upper (97.5%) bounds of the prediction error. The most consistent three detectors for each number of samples by average rank are in bold.

		Number of Training Examples			
		1000	2000	5000	10000
Top Five Detectors (Validation)	XGBOD (28%)	LOF (33%)	LOF (27%)	SVM (22%)	
	LOF (22%)	CBLOF (17%)	KNN (20%)	KNN (18%)	
	KNN (13%)	DeepSAD (16%)	SVM (13%)	LOF (14%)	
	CBLOF (11%)	KNN (15%)	CBLOF (11%)	CatB (13%)	
	FTTransformer (8%)	XGBOD (9%)	XGBOD (9%)	XGBOD (9%)	
Top Five Detectors (Test)	CBLOF (37%)	LOF (45%)	SVM (33%)	SVM (57%)	
	LOF (31%)	KNN (42%)	KNN (26%)	CatB (25%)	
	KNN (19%)	SVM (7%)	LOF (24%)	LOF (8%)	
	IForest (6%)	DeepSAD (3%)	CatB (13%)	KNN (6%)	
	CatB (6%)	XGBOD (1%)	DeepSAD (3%)	XGBOD (3%)	
Prediction Bounds	(-47.6, 1.6)	(-12.6, 1.5)	(-5.2, 1.5)	(-3.7, 1.3)	

(a) Results for S_1 (2 features).

		Number of Training Examples			
		1000	2000	5000	10000
Top Five Detectors (Validation)	LOF (25%)	LOF (36%)	XGBOD (37%)	XGBOD (54%)	
	KNN (22%)	KNN (29%)	LOF (26%)	LOF (19%)	
	CBLOF (15%)	XGBOD (12%)	KNN (21%)	KNN (9%)	
	XGBOD (14%)	CBLOF (11%)	DeepSAD (13%)	DeepSAD (8%)	
	DeepSAD (9%)	DeepSAD (5%)	CBLOF (3%)	CBLOF (7%)	
Top Five Detectors (Test)	LOF (42%)	LOF (53%)	LOF (48%)	XGBOD (80%)	
	KNN (35%)	KNN (44%)	KNN (26%)	LOF (9%)	
	CBLOF (22%)	XGBOD (3%)	XGBOD (26%)	KNN (7%)	
	XGBOD (0%)		CBLOF (0%)	CBLOF (3%)	
Prediction Bounds	(-13.1, 1.5)	(-9.4, 2.4)	(-4.1, 1.5)	(-2.2, 2.1)	

(b) Results for S_2 (10 features).

Table IX: Top five most frequently selected top detectors by validation and test AUCROC across different training dataset sizes (minimum of 199 simulations per sample size, thus 0% may be shown due to rounding). Percent frequency of detector selection is in brackets, rounded to nearest percent. Training anomaly rate is 0.5%.

example, kNN in S_1 at 10 000 samples has an expected variation of $(-1.5, 2.5)$. Therefore, if the validation AUCROC of kNN was measured at 97%, the testing AUCROC would be expected to be between 95.5% and 99.5%. In this way, the difference between the validation and testing metrics can be compared, with a smaller range corresponding to a more consistent detector. Based on the results in Table VIII, dataset size and feature size have a large impact on detector consistency.

As would be expected, the highest ranked detectors from Table VI are generally the most consistent detectors, and are also ranked highly in Table VIII. However, the top average rankings in Table VIII are not as high as the top average ranks in Table VI, indicating that many of the detectors are performing similarly on generalization.

Broadly, the unsupervised detectors tend to be the more consistent overall, simply because they do better on the smaller datasets.

Note that detectors do not always perform worse on the testing set than the training set, and the error can be quite symmetric for some methods. While this means detector performance has the potential to increase on the testing dataset (rather than only dropping), both drops and jumps in performance pose potential problems due to the requirement to select a detector based only on the validation metrics (as only the training dataset would be available in application). A higher estimated performance on validation means there is a greater chance than a poorer detector is selected for use, and a lower estimated performance may mean that the best detector is not

selected. Either case may lead to incorrect conclusions about the best detector.

In order to quantify this risk, including detector selection by validation, the best detector can be selected by validation AUCROC, whose performance can then be compared to the testing dataset. The prediction bounds for this strategy are reported in Table **IX**. These errors tend to be unsymmetrical, showing a greater tendency for AUCROC to drop between validation and testing than most detectors on their own (Table **VIII**).

Looking at the top detectors for each set, the best testing detectors are often the best selected based on validation, as would be expected, but there are some deviations. In several cases, deep learning methods such as DeepSAD and FTTransformer show up in validation, but not testing. Additionally, XGBOD only shows up as a top detector in S_2 ; it shows up in the validation selection for S_1 as well. This indicates that detection methods that utilize a large number of parameters are more likely to be incorrectly selected as the best detectors when they are not, which is likely contributing to the performance drop. This may be caused by the detectors overfitting to the validation dataset.

On the other side, SVM frequently shows up as a top detector for S_1 at 10 000 training examples, but is not in the most frequent detectors selected by validation. kNN and LOF both tend to be frequently selected as top performers.

In all cases, the error bounds for the prediction is very asymmetrical, with a large tendency to overestimate detection performance. So, while many individual detectors have the chance to increase or decrease in performance, the process of selecting the detector frequently leads to a performance drop. This could possibly be due to the cross-validation setup but the general process of applying a decision on which model to use, is itself part of the model creation process, and may contribute to over fitting.

However, the only way to avoid such a decision would be to have advance knowledge of which detector to use, or more information about the types of anomalies in the dataset. Increased knowledge of the problem may help in narrowing down the number of possible successful detection methods; lowering the risk of inadvertently selecting a poor detector. It can be noted that the performance of the detectors tends to become more consistent (Table **VIII**) and closer together (Table **VI**) as the dataset size increases, which helps to decrease the performance drop even if the best detector is not selected.

VI. CONCLUSION

In this simulation study, several anomaly detection algorithms were applied to two synthetic distributions under a wide range of training conditions. In this way, the experiment could be modified in ways that typical benchmark datasets could not be, in order to test the performance and generalization of the anomaly detectors. These results offer further insights into detector behaviour seen in previous research, and show why future researchers should carefully consider how the makeup (number of features/number of examples/anomaly rate) of the datasets they use for benchmarking may influence their final results.

To summarize the key findings:

- Only a small number of examples (30-50 examples) are required for top semi-supervised/supervised methods to match the performance of top unsupervised methods.
- At only 10 features, semi-supervised methods show significant increases in performance over supervised methods for the purpose of imbalanced classification.
- The total number of available faulty training examples is a key factor in selecting the best anomaly detector and more important than the anomaly rate.
- The false negative rate has a much higher MSE on generalization than AUCROC, and caution should be taken when evaluating model performance based on validation FNR.

By simulating realistic constraints and evaluating detectors across multiple training dataset sizes, these results provide practical guidance for deploying anomaly detection in industrial environments. They also underscore the importance of considering generalization error when selecting models for real-world applications, a characteristic that can't be tested in practice before a system is fully implemented. Future work may include the use of model-based simulations to create further testing datasets for specific problems, or the incorporation of more anomaly detection methods.

VII. ACKNOWLEDGMENTS

This work was supported in part by the Canada Research Chairs (CRC) Program under Project CRC-2020-0127 and in part by the Natural Sciences and Engineering Research Council of Canada (NSERC) Ford-Mitacs Alliance under Project ALLRP-590906-23. The authors would like to kindly thank Joanne Doucet for their valuable feedback on drafts of this article.

REFERENCES

[1] A. Kharitonov, A. Nahhas, M. Pohl, and K. Turowski, "Comparative analysis of machine learning models for anomaly detection in manufacturing," *Procedia Computer Science*, vol. 200, pp. 1288–1297, 2022. [Online]. Available: <https://linkinghub.elsevier.com/retrieve/pii/S1877050922003398>

[2] S. F. Chevtchenko, E. D. S. Rocha, M. C. M. D. Santos, R. L. Mota, D. M. Vieira, E. C. De Andrade, and D. R. B. De Araújo, "Anomaly Detection in Industrial Machinery Using IoT Devices and Machine Learning: A Systematic Mapping," *IEEE Access*, vol. 11, pp. 128 288–128 305, 2023. [Online]. Available: <https://ieeexplore.ieee.org/abstract/document/10318838>

[3] A. Melo, M. M. Câmara, and J. C. Pinto, "Data-Driven Process Monitoring and Fault Diagnosis: A Comprehensive Survey," *Processes*, vol. 12, no. 2, p. 251, Feb. 2024, number: 2 Publisher: Multidisciplinary Digital Publishing Institute. [Online]. Available: <https://www.mdpi.com/2227-9717/12/2/251>

[4] A. Liso, A. Cardellicchio, C. Patruno, M. Nitti, P. Ardino, E. Stella, and V. Renò, "A Review of Deep Learning-Based Anomaly Detection Strategies in Industry 4.0 Focused on Application Fields, Sensing Equipment, and Algorithms," *IEEE Access*, vol. 12, pp. 93 911–93 923, 2024. [Online]. Available: <https://ieeexplore.ieee.org/abstract/document/10587235>

[5] S. Han, X. Hu, H. Huang, M. Jiang, and Y. Zhao, "ADBench: Anomaly Detection Benchmark," *Advances in Neural Information Processing Systems*, vol. 35, pp. 32 142–32 159, Dec. 2022. [Online]. Available: https://proceedings.neurips.cc/paper_files/paper/2022/hash/cf93972b116ca5268827d575f2cc226b-Abstract-Datasets_and_Benchmarks.html

[6] M. Risdal, R. Prasanth, S. W. soundar, and W. Cukierski, "Bosch Production Line Performance," 2016. [Online]. Available: <https://kaggle.com/competitions/bosch-production-line-performance>

[7] F. Mauthe, S. Hagemeyer, and P. Zeiler, "Creation of Publicly Available Data Sets for Prognostics and Diagnostics Addressing Data Scenarios Relevant to Industrial Applications," *International Journal of Prognostics and Health Management*, vol. 12, no. 2, Nov. 2021. [Online]. Available: <https://papers.phmsociety.org/index.php/ijphm/article/view/3087>

[8] L. Wheat, M. V. Mohrenschildt, and S. Habibi, "Testing Bayes Error Rate Estimators in Difficult Situations Using Monte Carlo Simulations," *IEEE Access*, vol. 13, pp. 165 810–165 829, 2025. [Online]. Available: <https://ieeexplore.ieee.org/document/11162505>

[9] M.-A. Tnani, M. Feil, and K. Diepold, "Smart Data Collection System for Brownfield CNC Milling Machines: A New Benchmark Dataset for Data-Driven Machine Monitoring," *Procedia CIRP*, vol. 107, pp. 131–136, Jan. 2022. [Online]. Available: <https://www.sciencedirect.com/science/article/pii/S2212827122002384>

[10] N. Jourdan, L. Longard, T. Biegel, and J. Metternich, "Machine Learning For Intelligent Maintenance And Quality Control: A Review Of Existing Datasets And Corresponding Use Cases," in *2nd Conference on Production Systems and Logistics (CPSL 2021)*, D. Herberger and M. Hübner, Eds., 2021, publisher: Hannover : publish-Ing. [Online]. Available: <https://www.repo.uni-hannover.de/handle/123456789/11367>

[11] A. von Birgelen, D. Buratti, J. Mager, and O. Niggemann, "Self-Organizing Maps for Anomaly Localization and Predictive Maintenance in Cyber-Physical Production Systems," *Procedia CIRP*, vol. 72, pp. 480–485, Jan. 2018. [Online]. Available: <https://www.sciencedirect.com/science/article/pii/S221282711830307X>

[12] "PHM Data Challenge 2015," 2015. [Online]. Available: <https://phmsociety.org/>

conference/annual-conference-of-the-phm-society/annual-conference-of-the-prognostics-and-health-management-society-2015/phm-data-challenge-3/

[13] "Versatile Production System." [Online]. Available: <https://www.kaggle.com/datasets/inIT-OWL/versatileproductionsystem>

[14] "E-coating ultrafiltration maintenance dataset." [Online]. Available: <https://www.kaggle.com/datasets/boyangs444/process-data-for-predictive-maintenance>

[15] S. Martin del Campo Barraza, F. Sandin, and D. Strömbergsson, "Dataset concerning the vibration signals from wind turbines in northern Sweden," 2018. [Online]. Available: <https://urn.kb.se/resolve?urn=urn:nbn:se:ltu:diva-70730>

[16] Unknown, "APS Failure at Scania Trucks," 2016. [Online]. Available: <https://archive.ics.uci.edu/dataset/421>

[17] Backblaze, "Hard Drive Test Data," 2025. [Online]. Available: <https://www.backblaze.com/cloud-storage/resources/hard-drive-test-data>

[18] G. Xie, J. Wang, J. Liu, J. Lyu, Y. Liu, C. Wang, F. Zheng, and Y. Jin, "IM-IAD: Industrial Image Anomaly Detection Benchmark in Manufacturing," *IEEE Transactions on Cybernetics*, vol. 54, no. 5, pp. 2720–2733, May 2024. [Online]. Available: <https://ieeexplore.ieee.org/abstract/document/10443076>

[19] M. D. Xames, F. K. Torsha, and F. Sarwar, "A systematic literature review on recent trends of machine learning applications in additive manufacturing," *Journal of Intelligent Manufacturing*, vol. 34, no. 6, pp. 2529–2555, Aug. 2023. [Online]. Available: <https://doi.org/10.1007/s10845-022-01957-6>

[20] G. O. Campos, A. Zimek, J. Sander, R. J. G. B. Campello, B. Micenková, E. Schubert, I. Assent, and M. E. Houle, "On the evaluation of unsupervised outlier detection: measures, datasets, and an empirical study," *Data Mining and Knowledge Discovery*, vol. 30, no. 4, pp. 891–927, Jul. 2016. [Online]. Available: <https://doi.org/10.1007/s10618-015-0444-8>

[21] S. Matzka, "Explainable Artificial Intelligence for Predictive Maintenance Applications," in *2020 Third International Conference on Artificial Intelligence for Industries (AI4I)*, Sep. 2020, pp. 69–74. [Online]. Available: <https://ieeexplore.ieee.org/document/9253083/>

[22] Y. Pei and O. Zaiane, "A Synthetic Data Generator for Clustering and Outlier Analysis," University of Alberta Library, Tech. Rep., 2006. [Online]. Available: <https://doi.org/10.7939/R3B23S>

[23] C. Gao, X. Tan, J. Zhou, W. Ding, and W. Pedrycz, "Fuzzy Granule Density-Based Outlier Detection With Multi-Scale Granular Balls," *IEEE Transactions on Knowledge and Data Engineering*, vol. 37, no. 3, pp. 1182–1197, Mar. 2025. [Online]. Available: <https://ieeexplore.ieee.org/abstract/document/10821488>

[24] B. V. Sánchez Vinces, E. Schubert, A. Zimek, and R. L. F. Cordeiro, "A comparative evaluation of clustering-based outlier detection," *Data Mining and Knowledge Discovery*, vol. 39, no. 2, p. 13, Feb. 2025. [Online]. Available: <https://doi.org/10.1007/s10618-024-01086-z>

[25] L. Devroye, L. Györfi, and G. Lugosi, *A probabilistic theory of pattern recognition*. New York: Springer, 1996.

[26] K. Fukunaga and D. M. Hummels, "Bayes Error Estimation Using Parzen and k-NN Procedures," *IEEE Transactions on Pattern Analysis and Machine Intelligence*, vol. PAMI-9, no. 5, pp. 634–643, Sep. 1987. [Online]. Available: <https://ieeexplore.ieee.org/document/4767958>

APPENDIX A
ADDITIONAL RESULTS

		Number of Training Examples			
		1000	2000	5000	10000
US	True	TD (0.5, 1.7)	(0.6, 1.5)	(0.7, 1.3)	(0.8, 1.2)
	CBLOF	(0.5, 2.0)	(0.6, 1.6)	(0.8, 1.4)	(0.8, 1.2)
	DeepSVDD	(0.5, 1.8)	(0.6, 1.6)	(0.8, 1.4)	(0.8, 1.2)
	IForest	(0.4, 1.5)	(0.6, 1.4)	(0.8, 1.4)	(0.9, 1.4)
	KNN	(0.9, 100.0)	(0.6, 2.6)	(0.8, 1.7)	(0.8, 1.6)
	LOF	(0.6, 71.6)	(0.6, 4.4)	(0.8, 3.8)	(0.8, 2.6)
	OCSVM	(0.5, 1.8)	(0.6, 1.4)	(0.7, 1.3)	(0.8, 1.3)
SS	DeepSAD	(0.5, 1.9)	(0.7, 1.5)	(0.8, 1.4)	(0.8, 1.2)
	DevNet	(0.5, 1.6)	(0.6, 1.4)	(0.7, 1.3)	(0.8, 1.2)
	PReNet	(0.5, 1.7)	(0.6, 1.4)	(0.8, 1.3)	(0.8, 1.2)
	XGBOD	(0.7, 8.0)	(0.8, 5.5)	(0.5, 5.2)	(0.3, 3.6)
FS	CatB	(0.7, 2.3)	(0.7, 1.8)	(0.9, 1.5)	(0.9, 1.4)
	FTTransformer	(0.5, 1.9)	(0.6, 1.6)	(0.7, 1.3)	(0.8, 1.2)
	SVM	(0.5, 1.7)	(0.6, 1.4)	(0.7, 1.4)	(0.8, 1.2)
	XGB	(0.6, 3.7)	(0.7, 1.8)	(0.8, 1.5)	(0.9, 1.4)

(a) FPR by detector for S_1 .

		Number of Training Examples			
		1000	2000	5000	10000
US	True	TD (6.3, 9.1)	(6.6, 8.8)	(6.8, 8.3)	(7.0, 8.0)
	CBLOF	(8.7, 14.5)	(9.2, 14.5)	(9.4, 14.5)	(9.7, 15.3)
	DeepSVDD	(98.9, 99.9)	(98.9, 99.9)	(99.2, 99.9)	(99.8, 99.9)
	IForest	(23.1, 56.8)	(12.5, 41.1)	(9.2, 19.4)	(8.9, 10.9)
	KNN	(0.0, 9.3)	(7.2, 10.0)	(7.8, 9.5)	(8.0, 9.3)
	LOF	(6.7, 13.4)	(7.8, 11.4)	(8.1, 11.0)	(8.2, 9.5)
	OCSVM	(37.1, 99.9)	(37.8, 64.8)	(38.3, 40.7)	(38.4, 40.6)
SS	DeepSAD	(15.2, 33.4)	(11.6, 29.5)	(11.0, 27.3)	(11.5, 25.5)
	DevNet	(28.6, 74.1)	(28.1, 62.6)	(28.0, 43.0)	(27.9, 35.2)
	PReNet	(29.3, 69.6)	(28.2, 63.1)	(27.8, 39.4)	(28.2, 33.7)
	XGBOD	(7.2, 18.3)	(6.8, 13.7)	(6.6, 14.0)	(6.8, 13.2)
FS	CatB	(17.8, 61.7)	(12.5, 49.0)	(11.3, 25.9)	(10.5, 18.4)
	FTTransformer	(15.3, 69.0)	(13.6, 47.3)	(12.2, 30.3)	(10.0, 19.4)
	SVM	(31.8, 100.0)	(11.2, 77.6)	(9.3, 26.6)	(8.9, 18.1)
	XGB	(43.1, 85.9)	(33.7, 64.5)	(17.2, 38.4)	(13.0, 26.9)

(b) FNR by detector for S_1 .Table X: Results from simple anomaly predictor for S_1 .

		Number of Training Examples				
		1000	2000	5000	10000	
US	True	TD	(0.5, 1.6)	(0.7, 1.5)	(0.7, 1.4)	(0.8, 1.2)
		CBLOF	(0.6, 2.2)	(0.6, 1.6)	(0.7, 1.4)	(0.8, 1.3)
		DeepSVDD	(0.5, 1.7)	(0.6, 1.5)	(0.7, 1.3)	(0.8, 1.2)
		IForest	(0.4, 1.8)	(0.6, 1.5)	(0.7, 1.3)	(0.8, 1.2)
		KNN	(0.6, 100.0)	(0.6, 2.2)	(0.7, 1.8)	(0.8, 1.7)
		LOF	(0.6, 6.8)	(0.6, 4.8)	(0.7, 2.4)	(0.8, 1.5)
		OCSVM	(0.6, 2.0)	(0.6, 1.6)	(0.7, 1.4)	(0.8, 1.3)
		DeepSAD	(0.9, 2.6)	(0.8, 2.0)	(0.8, 1.5)	(0.9, 1.3)
		DevNet	(0.5, 1.9)	(0.6, 1.6)	(0.7, 1.3)	(0.8, 1.2)
		PReNet	(0.6, 1.9)	(0.7, 1.6)	(0.8, 1.4)	(0.8, 1.3)
SS		XGBOD	(1.0, 9.7)	(0.9, 6.3)	(0.7, 4.2)	(0.7, 4.1)
		CatB	(1.3, 3.1)	(1.2, 2.5)	(1.2, 2.1)	(1.2, 1.8)
		FTTransformer	(0.9, 2.5)	(1.0, 2.2)	(1.0, 1.9)	(1.1, 1.7)
		SVM	(0.5, 3.6)	(0.6, 1.9)	(0.7, 1.4)	(0.8, 1.2)
		XGB	(0.8, 2.1)	(0.9, 2.0)	(1.1, 1.8)	(1.2, 1.7)

(a) FPR by detector for S_2 .

		Number of Training Examples				
		1000	2000	5000	10000	
US	True	TD	(11.8, 20.1)	(12.6, 18.5)	(13.0, 17.6)	(13.8, 17.1)
		CBLOF	(22.0, 35.9)	(24.3, 36.6)	(25.6, 36.7)	(21.2, 29.1)
		DeepSVDD	(98.8, 100.0)	(98.9, 100.0)	(98.9, 100.0)	(99.0, 100.0)
		IForest	(53.2, 83.9)	(50.3, 73.4)	(46.9, 63.2)	(43.6, 60.8)
		KNN	(0.0, 29.3)	(19.7, 28.3)	(21.2, 26.8)	(21.6, 25.9)
		LOF	(16.3, 30.6)	(19.6, 28.9)	(21.4, 27.0)	(21.7, 26.4)
		OCSVM	(27.4, 40.8)	(29.6, 39.1)	(31.1, 37.0)	(31.7, 36.1)
		DeepSAD	(48.4, 67.5)	(44.5, 63.4)	(41.3, 60.3)	(35.5, 51.0)
		DevNet	(70.6, 88.6)	(66.4, 83.2)	(58.3, 73.3)	(51.9, 66.8)
		PReNet	(67.0, 87.1)	(63.4, 80.7)	(54.1, 71.6)	(49.1, 64.7)
SS		XGBOD	(14.3, 43.2)	(12.6, 30.4)	(11.6, 28.2)	(10.7, 25.1)
		CatB	(35.6, 70.5)	(43.3, 65.2)	(43.7, 62.7)	(35.3, 49.8)
		FTTransformer	(72.6, 89.4)	(65.7, 87.1)	(56.6, 82.3)	(48.5, 72.7)
		SVM	(34.9, 98.9)	(37.3, 91.2)	(35.4, 67.3)	(29.7, 52.0)
		XGB	(81.7, 93.0)	(72.3, 84.3)	(53.0, 68.8)	(40.8, 52.6)

(b) FNR by detector for S_2 .Table XI: Results from simple anomaly predictor for S_2 .